

Cluster Fragmentation and Facile Cleavage of Phenyl Groups from the SnPh_3 Ligand in Reactions of $\text{Os}_3(\text{CO})_{11}(\text{SnPh}_3)(\mu\text{-H})$ with CO and HSnPh_3

Richard D. Adams,* Burjor Captain, and Lei Zhu

Department of Chemistry and Biochemistry, University of South Carolina,
Columbia, South Carolina 29208

Received April 12, 2006

Two new cluster complexes, $\text{Os}_3(\text{CO})_{12}(\text{Ph})(\mu_3\text{-SnPh})$, **8** (35% yield), and $\text{Os}_4(\text{CO})_{16}(\mu_4\text{-Sn})$, **9** (10% yield), were formed when the complex $\text{Os}_3(\text{CO})_{11}(\text{SnPh}_3)(\mu\text{-H})$, **6**, was heated to reflux in toluene solvent under a CO atmosphere. Compound **8** was transformed to **9** in 28% yield when a solution in octane solvent was heated to reflux under a CO atmosphere. Biphenyl was a coproduct in this reaction. Compound **8** contains three osmium atoms with a triply bridging SnPh group. The triosmium cluster has opened and there is only one Os–Os bond between the three osmium atoms. Compound **9** contains two $\text{Os}_2(\text{CO})_8$ groups held together by a central quadruply bridging tin atom, giving an overall bow-tie structure for the five metal atoms. Two other new compounds, $\text{Os}_2(\text{CO})_6(\mu\text{-SnPh}_2)_2(\text{SnPh}_3)_2$, **10**, and $\text{HOs}(\text{CO})_4(\text{SnPh}_3)$, **11**, were formed in 51% and 20% yields, respectively, from the reaction of **6** with HSnPh_3 . Compound **10** contains only two osmium atoms linked by an Os–Os bond and two bridging SnPh_2 ligands. Each osmium atom also contains one terminal SnPh_3 ligand. Compound **11** contains only one osmium atom. It has one SnPh_3 ligand and a hydrido ligand in *cis* position in the six-coordinate pseudo-octahedral complex. All four new compounds were characterized by single-crystal X-ray diffraction analysis.

Introduction

Cleavage of phenyl groups from the heteroatoms of phenyl-containing ligands is an important transformation of metal complexes¹ that can lead to catalyst deactivation when it happens in complexes being used for homogeneous catalysis.² Tin is widely used as a modifier and promoter of homogeneous and heterogeneous catalysts.^{3–5} The stepwise hydrogenolysis of tin–carbon bonds of tetraalkyltin compounds is used to produce tin alloys of platinum nanoparticles.⁶ There is evidence that tin can assist in the binding of metallic nanoparticles to oxide supports of heterogeneous catalysts.⁷

In recent work we have shown that reactions of Ph_3SnH with metal carbonyl cluster complexes can lead to polynuclear metal

carbonyl complexes containing large numbers of SnPh_2 ligands of the type **a** by cleavage of a phenyl group that is eliminated as benzene.^{8–10} For example, the reaction of $\text{Ru}_5(\text{CO})_{15}(\mu_5\text{-C})$ with Ph_3SnH at 125 °C yielded the complex $\text{Ru}_5(\text{CO})_{10}(\text{SnPh}_3)(\mu\text{-SnPh}_2)_4(\mu_5\text{-C})(\mu\text{-H})$, **1**, containing five tin ligands; four are bridging SnPh_2 groups.⁸ Reactions of $\text{Rh}_4(\text{CO})_{12}$ and $\text{Ir}_4(\text{CO})_{12}$ with Ph_3SnH yielded the M_3Sn_6 complexes $\text{M}_3(\text{CO})_6(\mu\text{-SnPh}_2)_3(\text{SnPh}_3)_3$, **2** (M = Rh) and **3** (M = Ir), respectively, containing three bridging SnPh_2 ligands and three terminal SnPh_3 ligands.⁹ Compound **2** reacts still further with Ph_3SnH to yield the $\text{Rh}_3\text{-Sn}_8$ complex $\text{Rh}_3(\text{CO})_3(\text{SnPh}_3)_3(\mu\text{-SnPh}_2)_3(\mu_3\text{-SnPh})_2$, **4**, which contains three terminal SnPh_3 ligands, three edge-bridging SnPh_2 ligands, and the first examples of triply bridging SnPh ligands of the type **b**.⁹ Cleavage of phenyl groups from the SnPh_3 ligand in $\text{Ru}_5(\text{CO})_{11}(\text{C}_6\text{H}_6)(\text{SnPh}_3)(\mu\text{-H})(\mu_5\text{-C})$ yielded the complex $\text{Ru}_5(\text{CO})_{11}(\text{C}_6\text{H}_6)(\mu_4\text{-SnPh})(\mu_3\text{-CPh})$, **5**, containing the first example of a quadruply bridging SnPh ligand of the type **c**.^{8a}

* To whom correspondence should be addressed. E-mail: Adams@mail.chem.sc.edu.

(1) (a) Watson, W. H.; Wu, G.; Richmond, M. G. *Organometallics* **2006**, 25, 930. (b) Gainsford, G. J.; Guss, J. M.; Ireland, P. R.; Mason, R.; Bradford, C. W.; Nyholm, R. S. *J. Organomet. Chem.* **1972**, 40, C70. (c) Bradford, C. W.; Nyholm, R. S.; Gainsford, G. J.; Guss, J. M.; Ireland, P. R.; Mason, R. *Chem. Commun.* **1972**, 87.

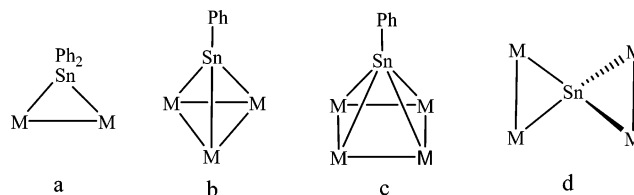
(2) Garrou, P. E. *Chem. Rev.* **1985**, 85, 171.

(3) (a) Burch, R. *J. Catal.* **1981**, 71, 348. (b) Burch, R.; Garla, L. C. *J. Catal.* **1981**, 71, 360. (c) Srinivasan, R.; Davis, B. H. *Platinum Metals Rev.* **1992**, 36, 151. (d) Fujikawa, T.; Ribeiro, F. H.; Somorjai, G. A. *J. Catal.* **1998**, 178, 58. (e) Llorca, J.; Homs, N.; Leon, J.; Sales, J.; Fierro, J. L. G.; Ramirez de la Piscina, P. *Appl. Catal. A: Gen.* **1999**, 189, 77. (f) Recchia, S.; Dossi, C.; Poli, N.; Fusi, A.; Sordelli, L.; Psaro, R. *J. Catal.* **1999**, 184, 1.

(4) (a) Huber, G. W.; Shabaker, J. W.; Dumesic, J. A. *Science* **2003**, 300, 2075. (b) Holt, M. S.; Wilson, W. L.; Nelson, J. H. *Chem. Rev.* **1989**, 89, 11. (c) Parshall, G. W. *J. Am. Chem. Soc.* **1972**, 94, 8716.

(5) Johnson, B. F. G.; Raynor, S. A.; Brown, D. B.; Shephard, D. S.; Mashmeyer, T.; Thomas, J. M.; Hermans, S.; Raja, R.; Sankar, G. *J. Mol. Catal. A: Chem.* **2002**, 182–183, 89.

(6) (a) Candy, J.-P.; Corperet, C.; Basset, J.-M. *Top. Organomet. Chem.* **2005**, 16, 151. (b) Lesage, P.; Candy, J.-P.; Hirigoyen, C.; Humblot, F.; Lecote, M.; Basset, J.-P. *J. Mol. Catal.* **1996**, 112, 303. (c) Chupin, C.; Candy, J.-P.; Corperet, C.; Basset, J.-M. *Catal. Today* **2003**, 79–80, 15.



(7) (a) Hermans, S.; Raja, R.; Thomas, J. M.; Johnson, B. F. G.; Sankar, G.; Gleeson, D. *Angew. Chem., Int. Ed.* **2001**, 40, 1211. (b) Hungria, A. B.; Raja, R.; Adams, R. D.; Captain, B.; Thomas, J. M.; Midgley, P. A.; Golvenko, V.; Johnson, B. F. G. *Angew. Chem. Int. Ed.* **2006**, in press.

(8) Adams, R. D.; Captain, B.; Fu, W.; Smith, M. D. *Inorg. Chem.* **2002**, 41, 5593. (b) Adams, R. D.; Captain, B.; Fu, W.; Smith, M. D. *Inorg. Chem.* **2002**, 41, 2302.

(9) Adams, R. D.; Captain, B.; Smith, J. L., Jr.; Hall, M. B.; Beddie, C. L.; Webster, C. E. *Inorg. Chem.* **2004**, 43, 7576.

(10) Adams, R. D.; Captain, B.; Zhu, L. *Organometallics* **2006**, 25, 2049.

We have recently obtained the complexes $\text{Os}_3(\text{CO})_{11}(\text{SnPh}_3)(\mu\text{-H})$, **6**, and $\text{Os}_3(\text{CO})_9(\mu\text{-SnPh}_2)_3$, **7**, from the reaction of $\text{Os}_3(\text{CO})_{12}$ with Ph_3SnH .¹⁰ Compound **6** has also been obtained in a better yield from the reaction of the more reactive triosmium derivative $\text{Os}_3(\text{CO})_{11}(\text{NCMe})$ with Ph_3SnH .¹¹ We have now investigated the cleavage of phenyl groups from the SnPh_3 ligand in **6**. We have found that *all* three phenyl groups can be cleaved from the tin atom with the formation of the new “bow-tie” cluster complex $\text{Os}_4(\text{CO})_{16}(\mu_4\text{-Sn})$, which contains a naked tin atom of the type **d** serving as a bridge between two $\text{Os}_2(\text{CO})_8$ groups.

Experimental Section

General Data. All the reactions were performed under a nitrogen atmosphere using standard Schlenk techniques. Reagent grade solvents were dried by standard procedures and were freshly distilled prior to use. Infrared spectra were recorded on an AVATAR 360 FT-IR spectrophotometer. ^1H NMR was recorded on a Varian Mercury 300 spectrometer operating at 300 MHz. Mass spectrometric measurements performed by direct exposure probe using electron impact ionization (EI) were made on a VG 70S instrument. Ph_3SnH was purchased from Aldrich and was used without further purification. $\text{Os}_3(\text{CO})_{11}(\text{SnPh}_3)(\mu\text{-H})$ was prepared according to the previously reported procedure.^{10,11} Product separations were performed by TLC in air on Analtech 0.25 and 0.5 mm silica gel 60 Å F_{254} glass plates.

Preparation of $\text{Os}_3(\text{CO})_{12}(\text{Ph})(\mu_3\text{-SnPh})$, **8, and $\text{Os}_4(\text{CO})_{16}(\mu_4\text{-Sn})$, **9**.** A 50 mg amount of **6** (0.041 mmol) dissolved in 20 mL of toluene was heated to reflux under a slow purge of CO for 10 h. The products were purified by TLC on silica gel using a 6:1 hexane–methylene chloride solvent mixture to yield in order of elution 5.0 mg (10% yield) of **9** and 17 mg (35% yield) of **8**. Spectral data for **8**: IR ν_{CO} (cm^{-1} in CH_2Cl_2): 2128 (w), 2102 (m), 2066 (s), 2048 (m), 2029 (m), 2017 (m), 1996 (w, sh), 1981 (w, sh). ^1H NMR (in CDCl_3): δ 6.88–7.70 (m, 10H, Ph). EI-MS m/z : 1180 with ions corresponding to consecutive loss of 12 CO ligands and the two phenyl groups. For **9**: IR ν_{CO} (cm^{-1} in CH_2Cl_2): 2095 (m), 2069 (vs), 2027 (s), 2005 (m). EI-MS m/z : 1328 with ions corresponding to consecutive loss of 16 CO ligands.

Conversion of **6 to **8** and **9** under CO (110 psi).** A 16 mg amount of **6** (0.013 mmol) was dissolved in 2 mL of toluene- d_8 . ^1H NMR of this solution showed multiple resonances in the region δ 7.15–7.76, corresponding to the protons on the phenyl rings. The solution was then sealed in a stainless steel Parr pressure reactor under CO atmosphere (100 psi) and placed in an oil bath at 130 °C for 2 h. The Parr reactor was then cooled to room temperature. ^1H NMR of the reaction mixture showed a resonance at δ 7.134, indicating the formation of benzene during the reaction. Compounds **8** and **9** were generated in 20% and 16% yields, respectively.

Conversion of **8 to **9**.** A 20 mg amount of **8** (0.017 mmol) was dissolved in 10 mL of octane in a 50 mL three-neck flask. The solution was heated to reflux under CO atmosphere (1 atm) for 2 h. The solvent was removed in vacuo, and the products were purified by TLC using a 6:1 hexane–methylene chloride solvent mixture to yield 5.8 mg (28%) of **9** and 0.9 mg (34%) of biphenyl.

Preparation of $\text{Os}_2(\text{CO})_6(\mu_2\text{-SnPh}_2)_2(\text{SnPh}_3)_2$, **10, and $\text{HOs}(\text{CO})_4\text{SnPh}_3$, **11**.** An 11 mg amount of **6** (0.0093 mmol) was dissolved in 10 mL of toluene in a 50 mL three-neck flask. An excess amount of HSnPh_3 was added, and the reaction was heated to reflux for 1 h. The solvent was removed in vacuo, and the products were purified by TLC on silica gel using a 6:1 hexane–methylene chloride solvent mixture to yield in order of elution 1.2 mg (20% yield) of **11** and 8.5 mg (51% yield) of **10**. Spectral data

for **10**: IR ν_{CO} (cm^{-1} in CH_2Cl_2): 2051 (m), 2006 (s), 1991 (m, sh). ^1H NMR (in CDCl_3): δ 7.08–7.39 (m, 50H, Ph). EI-MS m/z : 1794, and the observed isotope pattern is the same as the theoretical isotope pattern. Ions corresponding to loss of phenyl and CO ligands are also observed. Spectral data for **11**: IR ν_{CO} (cm^{-1} in CH_2Cl_2): 2125 (m), 2061 (m), 2038 (s). ^1H NMR (in CDCl_3): δ 7.27–7.62 (m, 15H, Ph), δ –8.94 (s, 1H, $^2J_{\text{Sn}^{117}\text{-H}} = 55.5$ Hz, $^2J_{\text{Sn}^{119}\text{-H}} = 57.9$ Hz). EI-MS m/z : 654, and the observed isotope pattern is the same as the theoretical isotope pattern. Ions corresponding to loss of benzene, CO, and phenyl ligands are also observed.

Reaction of **8 with HSnPh_3 .** A 9.5 mg amount of **8** (0.0081 mmol) and 8.5 mg of HSnPh_3 (0.024 mmol) were dissolved in 10 mL of toluene in a 50 mL three-neck flask. The solution was heated to reflux for 2.5 h. The solvent was removed in vacuo, and the products were purified by TLC by using a 6:1 hexane–methylene chloride solvent mixture to yield 1.4 mg (27%) of **11** and 2.2 mg (16%) of **10**. A trace amount of **9** (<1 mg) was also detected.

Crystallographic Analyses. Colorless single crystals of **8** suitable for diffraction analysis were grown by slow evaporation of solvent from a benzene–octane solution at 8 °C. Light yellow single crystals of **9** suitable for diffraction analysis were grown by slow evaporation of solvent from a CH_2Cl_2 –hexane solution at 8 °C. Orange single crystals of **10** were grown by slow evaporation of solvent from a benzene–octane solution at 8 °C. Colorless single crystals of **11** were grown from a solution in a CH_2Cl_2 –hexane solvent mixture by cooling to –20 °C. The data crystals used in the analyses were glued onto the end of a thin glass fiber. X-ray intensity data were measured using a Bruker SMART APEX CCD-based diffractometer using Mo $K\alpha$ radiation ($\lambda = 0.71073$ Å). The raw data frames were integrated with the SAINT+ program by using a narrow-frame integration algorithm.¹² Corrections for the Lorentz and polarization effects were also applied by SAINT. An empirical absorption correction based on the multiple measurement of equivalent reflections was applied by using the program SADABS. All structures were solved by a combination of direct methods and difference Fourier syntheses and refined by full-matrix least-squares on F^2 , by using the SHELXTL software package.¹³ Crystal data, data collection parameters, and results of the structural analyses for compound **8–11** are listed in Tables 1 and 2. For each structure all non-hydrogen atoms were refined with anisotropic displacement parameters. The hydrogen atoms on all phenyl rings were placed in geometrically idealized positions and included as standard riding atoms.

Compound **8** crystallized in the triclinic crystal system. The space group $P\bar{1}$ was assumed and confirmed by the successful solution and refinement of the structure.

Compound **9** crystallized in the monoclinic crystal system. The systematic absences in the intensity data were consistent with the space groups $C2/c$ and Cc . The former space group was chosen and confirmed by the successful solution and refinement of the structure.

Compound **10** crystallized in the triclinic crystal system. The space group $P\bar{1}$ was assumed and confirmed by the successful solution and refinement of the structure. The molecule is crystallographically centrosymmetrical and contains one-half of the formula equivalent of the molecule in the asymmetric crystal unit. Also, one molecule of benzene from the crystallization solvent was cocrystallized in the asymmetric unit.

Compound **11** crystallized in the triclinic crystal system. The space group $P\bar{1}$ was assumed and confirmed by the successful solution and refinement of the structure. The hydride ligand was located and refined with an isotropic thermal parameter.

(12) SAINT+, version 6.2a; Bruker Analytical X-ray Systems, Inc.: Madison, WI, 2001.

(13) Sheldrick, G. M. SHELXTL, version 6.1; Bruker Analytical X-ray Systems, Inc.: Madison, WI, 1997.

(11) Burgess, K.; Guerin, C.; Johnson, B. F. G.; Lewis, J. J. *Organomet. Chem.* **1985**, *295*, C3.

Table 1. Crystallographic Data for Compounds **8** and **9**

	8	9
empirical formula	$\text{Os}_3\text{SnO}_{12}\text{C}_{24}\text{H}_{10}$	$\text{Os}_4\text{SnO}_{16}\text{C}_{16}$
fw	1179.61	1327.65
cryst syst	triclinic	monoclinic
lattice params		
<i>a</i> (Å)	9.4672(5)	32.3449(12)
<i>b</i> (Å)	9.5559(5)	10.1687(4)
<i>c</i> (Å)	18.1476(9)	17.0856(6)
α (deg)	89.988(1)	90
β (deg)	81.515(1)	110.1970(10)
γ (deg)	64.473(1)	90
<i>V</i> (Å ³)	1461.59(13)	5274.0(3)
space group	<i>P</i> 1	<i>C</i> 2/ <i>c</i>
<i>Z</i> value	2	8
ρ_{calc} (g/cm ³)	2.680	3.344
$\mu(\text{Mo K}\alpha)$ (mm ⁻¹)	13.900	20.207
temperature (K)	293(2)	294(2)
$2\theta_{\text{max}}$ (deg)	56.6	56.6
no. obsd (<i>I</i> > 2 σ (<i>I</i>))	5438	5106
no. params	361	334
goodness of fit	1.043	1.053
max. shift in cycle	0.001	0.000
residuals: ^a <i>R</i> ₁ ; <i>wR</i> ₂	0.0349; 0.0722	0.0354; 0.0693
absorp corr.	SADABS	SADABS
max./min.	1.000/0.519	1.000/0.595
largest peak in final diff map (e ⁻ /Å ³)	1.586	3.052

$$^a R_1 = \frac{\sum_{hk\ell} (|F_{\text{obs}}| - |F_{\text{calc}}|) / \sum_{hk\ell} |F_{\text{obs}}|}{\sum_{hk\ell} |F_{\text{obs}}|}; wR_2 = \frac{[\sum_{hk\ell} w(|F_{\text{obs}}| - |F_{\text{calc}}|)^2 / \sum_{hk\ell} w |F_{\text{obs}}|^2]^{1/2}}{[\sum_{hk\ell} w |F_{\text{obs}}|^2]^{1/2}}, w = 1/\sigma^2(F_{\text{obs}}); \text{GOF} = \frac{[\sum_{hk\ell} w(|F_{\text{obs}}| - |F_{\text{calc}}|)^2 / (n_{\text{data}} - n_{\text{var}})]^{1/2}}{[\sum_{hk\ell} w |F_{\text{obs}}|^2]^{1/2}}.$$

Table 2. Crystallographic Data for Compounds **10** and **11**

	10	11
empirical formula	$\text{Os}_2\text{Sn}_4\text{O}_6\text{C}_{66}\text{H}_{50} \cdot 2\text{C}_6\text{H}_6$	$\text{OsSnO}_4\text{C}_{22}\text{H}_{16}$
fw	1950.44	653.24
cryst syst	triclinic	triclinic
lattice params		
<i>a</i> (Å)	11.2240(3)	9.6670(4)
<i>b</i> (Å)	11.3303(3)	10.8704(4)
<i>c</i> (Å)	16.0970(4)	11.2785(4)
α (deg)	93.721(1)	67.827(1)
β (deg)	109.943(1)	88.862(1)
γ (deg)	110.146(1)	83.898(1)
<i>V</i> (Å ³)	1767.59(8)	1091.06(7)
space group	<i>P</i> 1	<i>P</i> 1
<i>Z</i> value	1	2
ρ_{calc} (g/cm ³)	1.832	1.988
$\mu(\text{Mo K}\alpha)$ (mm ⁻¹)	5.022	6.985
temperature (K)	293(2)	294(2)
$2\theta_{\text{max}}$ (deg)	55.8	56.6
no. obsd (<i>I</i> > 2 σ (<i>I</i>))	7724	4947
no. params	406	257
goodness of fit	1.149	1.051
max. shift in cycle	0.002	0.002
residuals: ^a <i>R</i> ₁ ; <i>wR</i> ₂	0.0198; 0.0496	0.0195; 0.0469
absorp corr.	SADABS	SADABS
max./min.	1.000/0.773	1.000/0.708
largest peak in final diff map (e ⁻ /Å ³)	0.962	1.298

$$^a R_1 = \frac{\sum_{hk\ell} (|F_{\text{obs}}| - |F_{\text{calc}}|) / \sum_{hk\ell} |F_{\text{obs}}|}{\sum_{hk\ell} |F_{\text{obs}}|}; wR_2 = \frac{[\sum_{hk\ell} w(|F_{\text{obs}}| - |F_{\text{calc}}|)^2 / \sum_{hk\ell} w |F_{\text{obs}}|^2]^{1/2}}{[\sum_{hk\ell} w |F_{\text{obs}}|^2]^{1/2}}, w = 1/\sigma^2(F_{\text{obs}}); \text{GOF} = \frac{[\sum_{hk\ell} w(|F_{\text{obs}}| - |F_{\text{calc}}|)^2 / (n_{\text{data}} - n_{\text{var}})]^{1/2}}{[\sum_{hk\ell} w |F_{\text{obs}}|^2]^{1/2}}.$$

Results and Discussion

Two new cluster complexes, $\text{Os}_3(\text{CO})_{12}(\text{Ph})(\mu_3\text{-SnPh})$, **8** (35% yield), and $\text{Os}_4(\text{CO})_{16}(\mu_4\text{-Sn})$, **9** (10% yield), were formed when the complex $\text{Os}_3(\text{CO})_{11}(\text{SnPh}_3)(\mu\text{-H})$, **6**, was heated to reflux in toluene solvent under a CO atmosphere for 10 h. Benzene was observed as a coproduct from this reaction. Compound **8** was characterized by single-crystal X-ray diffraction analysis. An ORTEP diagram of the molecular structure of **8** is shown in Figure 1. The molecule contains three $\text{Os}(\text{CO})_4$ groups

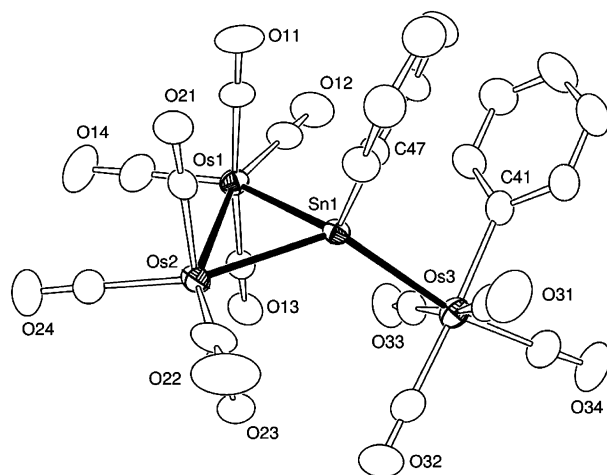


Figure 1. ORTEP diagram of $\text{Os}_3(\text{CO})_{12}(\text{Ph})(\mu_3\text{-SnPh})$, **8**, showing 30% probability thermal ellipsoids. Selected interatomic distances (Å) and angles (deg): $\text{Os}(1)\text{---}\text{Os}(2) = 3.0007(4)$, $\text{Os}(1)\text{---}\text{Sn}(1) = 2.7240(6)$, $\text{Os}(2)\text{---}\text{Sn}(1) = 2.7283(6)$, $\text{Os}(3)\text{---}\text{Sn}(1) = 2.7532(6)$, $\text{Os}(3)\text{---}\text{C}(41) = 2.172(9)$; $\text{Os}(1)\text{---}\text{Sn}(1)\text{---}\text{Os}(3) = 126.597(19)$, $\text{Os}(2)\text{---}\text{Sn}(1)\text{---}\text{Os}(3) = 128.81(2)$, $\text{C}(41)\text{---}\text{Os}(3)\text{---}\text{Sn}(1) = 82.8(2)$.

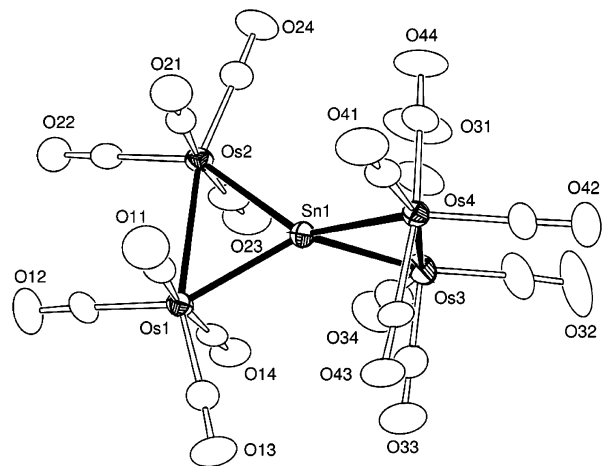


Figure 2. ORTEP diagram of $\text{Os}_4(\text{CO})_{16}(\mu_4\text{-Sn})$, **9**, showing 30% probability thermal ellipsoids. Selected interatomic distances (Å) and angles (deg): $\text{Os}(1)\text{---}\text{Os}(2) = 3.0081(5)$, $\text{Os}(1)\text{---}\text{Sn}(1) = 2.6927(7)$, $\text{Os}(2)\text{---}\text{Sn}(1) = 2.6883(7)$, $\text{Os}(3)\text{---}\text{Os}(4) = 3.0038(5)$, $\text{Os}(3)\text{---}\text{Sn}(1) = 2.6983(7)$, $\text{Os}(4)\text{---}\text{Sn}(1) = 2.6797(7)$; $\text{Os}(4)\text{---}\text{Sn}(1)\text{---}\text{Os}(2) = 136.86(3)$, $\text{Os}(4)\text{---}\text{Sn}(1)\text{---}\text{Os}(1) = 135.85(2)$, $\text{Os}(2)\text{---}\text{Sn}(1)\text{---}\text{Os}(1) = 67.975(17)$, $\text{Os}(4)\text{---}\text{Sn}(1)\text{---}\text{Os}(3) = 67.907(18)$, $\text{Os}(2)\text{---}\text{Sn}(1)\text{---}\text{Os}(3) = 130.34(3)$, $\text{Os}(1)\text{---}\text{Sn}(1)\text{---}\text{Os}(3) = 130.32(2)$.

connected by a triply bridging SnPh group. There is only one $\text{Os}\text{---}\text{Os}$ bond, $\text{Os}(1)\text{---}\text{Os}(2) = 3.0007(4)$ Å, which connects two of the $\text{Os}(\text{CO})_4$ groups. There is a phenyl group σ -bonded to the third $\text{Os}(\text{CO})_4$ group, $\text{Os}(3)\text{---}\text{C}(41) = 2.172(9)$ Å. The $\text{Os}\text{---}\text{Sn}$ bond distances, $\text{Os}(1)\text{---}\text{Sn}(1) = 2.7240(6)$ Å, $\text{Os}(2)\text{---}\text{Sn}(1) = 2.7283(6)$ Å, $\text{Os}(3)\text{---}\text{Sn}(1) = 2.7532(6)$ Å, are slightly longer than the $\text{Os}\text{---}\text{Sn}$ distance to the SnPh_3 group in **6**, $\text{Os}(1)\text{---}\text{Sn}(1) = 2.6949(6)$ Å.¹⁰

Compound **8** is a precursor to **9**. It was transformed to **9** in 28% yield when a solution in octane solvent was heated to reflux under an atmosphere of CO. Biphenyl was observed as a coproduct from this reaction and was obtained in a yield (34%) that is similar to the yield of **9**. Compound **9** was also characterized by a single-crystal X-ray diffraction analysis, and an ORTEP diagram of its molecular structure is shown in Figure 2. Compound **9** contains two $\text{Os}_2(\text{CO})_8$ groups held together by a central quadruply bridging tin atom, giving an overall bow-tie structure for the five metal atoms. The complex has

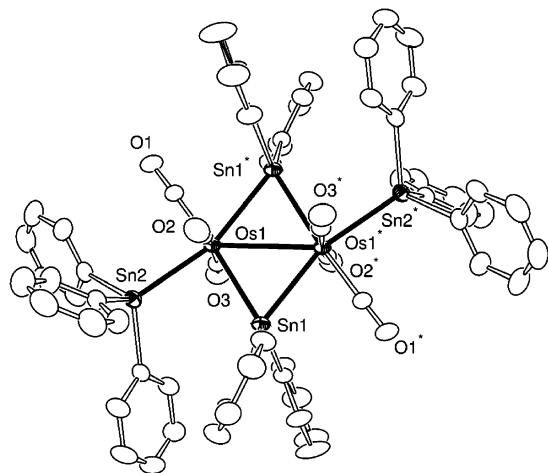


Figure 3. ORTEP diagram of $\text{Os}_2(\text{CO})_6(\mu\text{-SnPh}_2)_2(\text{SnPh}_3)_2$, **10**, showing 30% probability thermal ellipsoids. Selected interatomic distances (Å) and angles (deg) $\text{Os}(1)\text{---}\text{Os}(1^*) = 3.1471(2)$, $\text{Os}(1)\text{---}\text{Sn}(1) = 2.6789(2)$, $\text{Os}(1)\text{---}\text{Sn}(2) = 2.7253(2)$, $\text{Os}(1)\text{---}\text{Sn}(1^*) = 2.7593(2)$; $\text{Sn}(1)\text{---}\text{Os}(1)\text{---}\text{Sn}(1^*) = 109.301(6)$; $\text{Os}(2)\text{---}\text{Os}(1)\text{---}\text{Sn}(1^*) = 162.888(8)$, $\text{Sn}(2)\text{---}\text{Os}(1)\text{---}\text{Os}(1^*) = 142.214(7)$.

approximate D_{2d} symmetry, which is not crystallographically imposed. The Os–Os bond distances, $\text{Os}(1)\text{---}\text{Os}(2) = 3.0081(5)$ Å and $\text{Os}(3)\text{---}\text{Os}(4) = 3.0038(5)$ Å, are very similar to that in **8**. The four Os–Sn bond distances are slightly shorter than those in **8**, $\text{Os}(1)\text{---}\text{Sn}(1) = 2.6927(7)$ Å, $\text{Os}(2)\text{---}\text{Sn}(1) = 2.6883(7)$ Å, $\text{Os}(3)\text{---}\text{Sn}(1) = 2.6983(7)$ Å, $\text{Os}(4)\text{---}\text{Sn}(1) = 2.6797(7)$ Å, but are very similar to those in the compound $\text{Os}_3(\text{CO})_9(\mu\text{-H})_3(\mu_4\text{-Sn})\text{Os}_3(\text{CO})_{10}(\text{PET}_2\text{Ph})(\mu\text{-H})$, **10**, which contains a tin atom bridging the triangle of one Os_3 cluster with a bond to one osmium atom of a second triangular Os_3 cluster.¹⁴ Some related iron compounds containing similar quadruply bridging tin atoms have been reported, e.g., $\text{Fe}_2(\text{CO})_8(\mu_4\text{-Sn})\text{Fe}_2(\text{CO})_8$,¹⁵ $\text{Fe}_2(\text{CO})_8(\mu_4\text{-Sn})\text{Fe}_2(\text{CO})_7(\mu_4\text{-Sn})\text{Fe}_2(\text{CO})_8$,¹⁶ $[\text{NET}_4][\text{Fe}_2(\text{CO})_8(\mu_4\text{-Sn})\{\text{Fe}(\text{CO})_4\}_2]$,¹⁷ $\text{Fe}_2(\text{CO})_8(\mu_4\text{-Sn})\text{Fe}_3(\text{CO})_{11}$,¹⁸ and $[\text{Fe}_2(\text{CO})_8(\mu_3\text{-SnMe}_2)]_2(\mu_4\text{-Sn})$.¹⁹ These were obtained by a variety of different procedures.

When compound **6** was treated with Ph_3SnH , two new compounds, $\text{Os}_2(\text{CO})_6(\mu\text{-SnPh}_2)_2(\text{SnPh}_3)_2$, **10**, and $\text{HOs}(\text{CO})_4(\text{SnPh}_3)$, **11**, were formed in 51% and 20% yields, respectively. Both compounds were characterized crystallographically. An ORTEP diagram of the structure of **10** is shown in Figure 3. In the solid state, the structure of **10** is crystallographically centrosymmetrical. Each osmium atom contains one terminal SnPh_3 ligand, $\text{Os}(1)\text{---}\text{Sn}(2) = 2.7253(2)$ Å, and three linear terminal carbonyl ligands. The two SnPh_3 ligands have an overall *trans* geometry with respect to the Os–Os bond. The molecule contains two bridging SnPh_2 ligands positioned on opposite sides of the molecule. The $\text{Os}(1)\text{---}\text{Sn}(1^*)$ bond that is *trans* to the terminal SnPh_3 ligand is considerably longer than the Os–Sn bond that is terminal to a CO ligand, $\text{Os}(1)\text{---}\text{Sn}(1) = 2.6789(2)$ Å and $\text{Os}(1)\text{---}\text{Sn}(1^*) = 2.7593(2)$ Å. To obey the

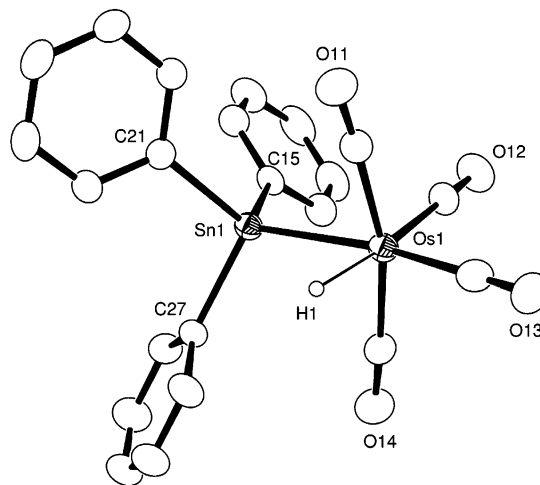


Figure 4. ORTEP diagram of $\text{HOs}(\text{CO})_4(\text{SnPh}_3)$, **11**, showing 30% probability thermal ellipsoids. Selected interatomic distances (Å) and angles (deg): $\text{Os}(1)\text{---}\text{Sn}(1) = 2.7382(2)$, $\text{Os}(1)\text{---}\text{H}(1) = 1.67(4)$, $\text{Os}(1)\text{---}\text{C}(11) = 1.944(3)$, $\text{Os}(1)\text{---}\text{C}(12) = 1.967(3)$, $\text{Os}(1)\text{---}\text{C}(13) = 1.948(3)$, $\text{Os}(1)\text{---}\text{C}(14) = 1.942(3)$; $\text{Sn}(1)\text{---}\text{Os}(1)\text{---}\text{H}(1) = 79.3(12)$.

18-electron configurations, the two osmium atoms should contain an Os–Os single bond. Although the Os–Os distance, $\text{Os}(1)\text{---}\text{Os}(1^*) = 3.1471(2)$ Å, is certainly short enough to be considered a bonding distance, it is considerably longer than the Os–Os bond distances in **8** and **9** and also in $\text{Os}_3(\text{CO})_{12}$, 2.877(3) Å;²⁰ $\text{Os}_3(\text{CO})_{12}$ has no bridging ligands. It is even longer than the three Os–Os bonds in **7**, $\text{Os}(1)\text{---}\text{Os}(2) = 2.9629(4)$ Å, $\text{Os}(1)\text{---}\text{Os}(3) = 2.9572(4)$ Å, $\text{Os}(2)\text{---}\text{Os}(3) = 2.9906(4)$ Å. We have found in previous studies that metal–metal bonds containing bridging SnPh_2 tend to be longer than the corresponding unbridged metal–metal bonds.^{9,21} Theoretical analyses have indicated that this is due to the presence of strong M–Sn bonding interactions that compete with the M–M bonding interactions.⁹ The Re–Re bond in the compound $\text{Re}_2(\text{CO})_8(\mu\text{-SnPh}_2)_2$ is also unusually long.²¹ Compound **10** is structurally similar to the related known ruthenium compound $\text{Ru}_2(\text{CO})_6(\mu\text{-SnMe}_2)_2(\text{SnMe}_3)_2$.²²

An ORTEP diagram of the structure of **11** is shown in Figure 4. Compound **11** contains only one osmium atom. It has a six-coordinate pseudo-octahedral coordination with four carbonyl ligands, and one SnPh_3 ligand and a hydrido ligand that are positioned *cis* to one another. The Os–Sn bond is very similar in length to that in **10**, $\text{Os}(1)\text{---}\text{Sn}(1) = 2.7382(2)$ Å. The hydrido ligand was located and refined crystallographically, $\text{Os}(1)\text{---}\text{H}(1) = 1.67(4)$ Å. Its resonance in the ¹H NMR spectrum exhibits the characteristic high-field shift, $\delta = -8.94$ (s, 1H), with two bond couplings to tin, $^2J_{\text{Sn}^{117}\text{-H}} = 55.5$ Hz, $^2J_{\text{Sn}^{119}\text{-H}} = 57.9$ Hz.

A summary of the transformations reported here is shown in Scheme 1. We have demonstrated that all of the phenyl groups can be cleaved from a triphenyltin ligand to produce a naked tin atom serving as a bridging ligand between four osmium atoms. All of the details of the mechanism of the formation of **8** and **9** from **6** are not yet known, but the formation of benzene and bridging SnPh_2 ligands were formed from reactions involving HSnPh_3 .⁸ In the present reaction, additional cleavages of the

(14) Leong, W. K.; Einstein, F. W. B.; Pomeroy, R. K. *J. Cluster Sci.* **1996**, *7*, 211.

(15) (a) Cotton, J. D.; Duckworth, J.; Knox, S. A. R.; Lindley, P. F.; Paul, I.; Stone, F. G. A.; Woodward, P. *J. Chem. Soc., Chem. Commun.* **1966**, 253. (b) Lindley, P. F.; Woodward, P. *J. Chem. Soc. A* **1967**, 382.

(16) Anema, S. G.; Mackay, K. M.; Nicholson, B. K. *Inorg. Chem.* **1989**, *28*, 3158.

(17) Cassidy, J. M.; Whitmire, K. H.; Kook, A. M. *J. Organomet. Chem.* **1993**, *456*, 61.

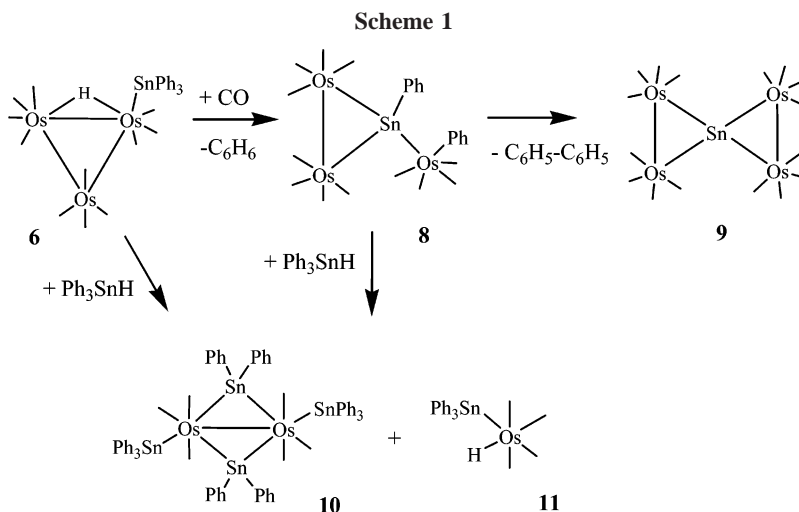
(18) Anema, S. G.; Mackay, K. M.; Nicholson, B. K. *J. Organomet. Chem.* **1989**, *372*, 25.

(19) Sweet, R. M.; Fritchie, C. J.; Schunn, R. A. *Inorg. Chem.* **1967**, *6*, 749.

(20) Churchill, M. R.; DeBoer, B. G. *Inorg. Chem.* **1977**, *16*, 878.

(21) (a) Adams, R. D.; Captain, B.; Herber, R. H.; Johansson, M.; Nowik, I.; Smith, J. L., Jr.; Smith, M. D. *Inorg. Chem.* **2005**, *44*, 6346. (b) Adams, R. D.; Captain, B.; Johansson, M.; Smith, J. L., Jr. *J. Am. Chem. Soc.* **2005**, *127*, 488.

(22) Watkins, S. F. *J. Chem. Soc. A* **1969**, 1552.



phenyl groups from the tin atom occur. In particular, in the formation of **8**, one phenyl group was also transferred from the tin atom to one of the osmium atoms. A CO ligand was also added, which led to an opening of the Os_3 cluster. Compounds **8** and **9** were also obtained when **6** was heated in the absence of CO, but the yields were much lower because of the lack of CO required for their formation. Compound **8** was transformed to **9**, which has no phenyl rings. Since there are no available hydrido ligands for the formation of benzene from **8**, the two phenyl rings were combined instead and were eliminated in the form of biphenyl. The number of $\text{Os}(\text{CO})_4$ groups was increased by one on going from **8** to **9**. The nature of this transformation is not clear. This could occur by transfer of an $\text{Os}(\text{CO})_4$ group from a second molecule of **8** or by an exchange of an $\text{Os}_2(\text{CO})_8$ group for an $\text{Os}(\text{CO})_4$ group from a second molecule of **8** in the course of the elimination of the biphenyl.

Compounds **10** and **11** were both obtained also from the reaction of **8** with HSnPh_3 . Indeed, the opening of the Os_3 triangle to form **8** may be the first step in the fragmentation process that leads to **10** and **11** in the reaction of **6** with HSnPh_3 .

The compounds that we have reported here show a sequence of steps for the incorporation of a naked tin into the tetraosmium complex **9**. Even though cluster fragmentation does occur in this reaction sequence, the nature of tin-carbon bond cleavages may be relevant to the incorporation of tin atoms into higher nuclearity clusters and transition metal nanoparticles from organotin reagents in general.^{4a,6} The facile cleavage of phenyl rings from phenyltin ligands may prove to be an effective route to new families of metal carbonyl cluster complexes containing naked bridging tin atoms. Tin-containing cluster complexes are now proving to be useful precursors to new supported bi- and trimetallic heterogeneous catalysts.⁷

Acknowledgment. This research was supported by the Office of Basic Energy Sciences of the U.S. Department of Energy under Grant No. DE-FG02-00ER14980.

Supporting Information Available: CIF files for each of the structural analyses are available. This material is available free of charge via the Internet at <http://pubs.acs.org>.

OM0603262